

# Robust Zero Energy Bound States Localized at Magnetic Impurities in Iron-based Superconductors

Kangjun Seo<sup>1</sup>, Jay D. Sau<sup>2</sup>, and Sumanta Tewari<sup>1</sup>

<sup>1</sup>*Department of Physics and Astronomy, Clemson University, Clemson, SC 29634*

<sup>2</sup>*Condensed Matter Theory Center and Joint Quantum Institute,  
Department of Physics, University of Maryland, College Park, Maryland 20742-4111*

(Dated: August 30, 2019)

We show that robust zero-energy bound states can be induced at magnetic impurities in iron-based superconductors with unconventional (sign-changed)  $s$ -wave pairing symmetry in the presence of spin-orbit coupling. The zero-energy bound states localized at the impurities are robust to applied magnetic fields and variation in the strength of the impurity potentials by the combined effects of spin-orbit coupling and the existence of low-energy sub-gap states inside the superconducting gap. This work provides an explanation to the puzzling recent observation of robust zero bias peaks observed in scanning tunneling microscopy experiments at magnetic impurities in iron-based superconductor  $\text{Fe}_{1+x}(\text{Te},\text{Se})$  where  $x$  is the concentration of magnetic impurities.

PACS numbers: 73.20.Hb, 74.20.-z, 74.70.Xa, 75.70.Tj

We are motivated by a recent scanning tunneling microscope (STM) observation of a robust zero bias conductance peak (un-split by an applied magnetic field  $\sim 8T$ ) induced at magnetic impurities in iron-based superconductor  $\text{Fe}_{1+x}(\text{Te},\text{Se})$ <sup>1</sup>. Zero- or low-energy sub-gap states bound to magnetic and/or non-magnetic impurities in superconductors are not unusual<sup>2-13</sup>. However, in spin-singlet superconductors [e.g.,  $s$ -wave ( $s_{++}$ ,  $s_{+-}$ -wave),  $d$ -wave, etc], the zero bias peaks localized at impurities are expected to split into a double peak structure on application of a magnetic field. Qualitatively, the splitting of the peak by a magnetic field is due to the fundamental two-fold spin degeneracy of Bogoliubov quasi-particle states in a singlet superconductor. Since the spin of the zero-energy bound states couples to a magnetic field via Zeeman coupling, the zero bias STM peak, if any, gives rise to a double peak structure by application of a magnetic field. Theoretically, a defect-induced zero-energy state can escape splitting when the state is non-degenerate. A non-degenerate zero energy bound state in a superconductor, on the other hand, is very unusual, and is commonly referred as a Majorana bound state (MBS) that can be realized in a topological superconductor<sup>14-16</sup>. This has led to the tantalizing conjecture of realizing a topological superconductor and MBS in iron-based superconductors induced by superconductivity, spin-orbit coupling (which may be induced by the heavy  $5p$  Te atoms in  $\text{Fe}_{1+x}(\text{Te},\text{Se})$ ), and local magnetic order induced by the magnetic impurities<sup>1</sup>.

In this paper we show that the robust zero-energy bound states localized at magnetic impurities in iron-based superconductor  $\text{Fe}_{1+x}(\text{Te},\text{Se})$  can be explained in terms of non-topological zero energy bound states which are, nonetheless, robust to perturbations such as Zeeman fields and variation of the strength of the impurity potential by the combined effects of spin-orbit coupling (SOC) and a finite density of low energy sub-gap states present at the impurity sites. As noted already in Ref. [1], unlike FeSe, the  $5p$  heavy Te atoms in  $\text{Fe}(\text{Te},\text{Se})$  has strong SOC and may induce the same in the conduction band of  $\text{Fe}(\text{Te},\text{Se})$  by modifying the band structure. The low-energy sub-gap states at the impurity sites are either a consequence of SOC (for large enough SOC, the system is a nodal superconductor) or may naturally arise from overlap

of the impurity-induced sub-gap states bound to nearby magnetic impurities in the superconductor. We note that the local density of states (LDOS) measured at the impurity sites in samples with a finite density of magnetic impurities indeed indicates a finite density of low-energy sub-gap quasiparticle states, in addition to a robust zero bias peak un-split by a magnetic field<sup>1</sup>. With this minimal, experimentally motivated, modeling of the band-structure we are able to show that a robust zero bias conductance peak is induced at magnetic impurities in iron-based superconductors provided the symmetry of the superconducting order parameter is sign-changing  $s_{+-}$ -wave. On the other hand, the conventional  $s_{++}$  pairing symmetry does not provide the robust zero-energy bound states at magnetic impurities, being strongly affected by the perturbation of a magnetic field even with spin-orbit coupling and a finite density of low energy quasi-particle states. Thus, our results, in addition to providing a consistent theoretical explanation of the puzzling observation of robust zero bias conductance peaks in iron-based superconductors (that has been described as a serious theoretical challenge in recent literature<sup>1</sup>), also helps in identifying the relevant symmetry of the superconducting order parameter as sign-changing  $s_{+-}$  wave.

We start with a mean-field Hamiltonian for the iron-based superconductor using the two-orbital model ( $d_{xz}$  and  $d_{yz}$ ) on the two-dimensional Fe square lattice<sup>17</sup>,

$$H = H_0 + H_{\text{mag}} + H_{\text{imp}}. \quad (1)$$

Here,  $H_0$  is the tight-binding Hamiltonian in the superconducting state, including intra- and inter-orbital hopping integrals

$$H_0 = \sum_{\mathbf{ij}\alpha\beta\sigma} t_{\mathbf{ij}}^{\alpha\beta} c_{\mathbf{i}\alpha\sigma}^\dagger c_{\mathbf{j}\beta\sigma} - \mu \sum_{\mathbf{i}\alpha\sigma} c_{\mathbf{i}\alpha\sigma}^\dagger c_{\mathbf{i}\alpha\sigma} + H_{\text{pair}}, \quad (2)$$

where  $c_{\mathbf{i}\alpha\sigma}^\dagger$  creates an electron with spin  $\sigma$  in the orbitals  $\alpha = 1$  ( $d_{xz}$ ) and  $2$  ( $d_{yz}$ ) at site  $\mathbf{i}$ . We choose the nearest-neighbor hopping matrix elements as  $t_{\mathbf{i}\pm\hat{x}}^{11} = t_{\mathbf{i}\pm\hat{y}}^{22} = t_1$ ,  $t_{\mathbf{i}\pm\hat{x}}^{11} = t_2 = -1.3t_1$ , and the next-nearest-neighbor hopping as  $t_{\mathbf{i}\pm(\hat{x}+\hat{y})}^{\alpha\alpha} = t_{\mathbf{i}\pm(\hat{x}-\hat{y})}^{\alpha\alpha} = t_3$ , and  $t_{\mathbf{i}\pm(\hat{x}+\hat{y})}^{\alpha\beta} = -t_{\mathbf{i}\pm(\hat{x}-\hat{y})}^{\alpha\beta} = t_4$  with  $t_3 = t_4 = 0.85t_1$ . We have taken  $t_1 = 10$  meV as the energy units and lattice constant  $a = 1$ . The chemical potential

$\mu = 1.65t_1$  is adjusted to give a fixed filling factor  $n_e \simeq 2.1$  per site.

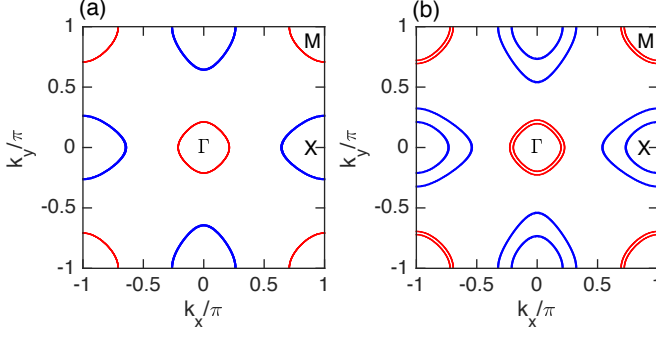


FIG. 1. (a) Fermi surfaces of the two-band model at  $\mu = 1.65t_1$  in the unfolded BZ, and (b) the fermi surfaces of the helicity bands in the presence of the Rashba-type SOC with  $v = 0.25t_1 = 2.5$  meV. The red pockets at  $\Gamma$  and  $M$  points represent the holelike pockets, and the blue pockets at  $X$  point represent the electronlike pockets. The SOC produces the additional Fermi surfaces with the same chemical potential.

The Fermi surfaces consist of the hole pockets at  $\Gamma$  and  $M$  points and the electron pocket at  $X$  point in the unfolded Brillouin Zone [Fig. 1(a)] with no SOC. The pairing Hamiltonian  $H_{\text{pair}}$  is given by

$$H_{\text{pair}} = \sum_{\mathbf{i}, \mathbf{j}} \Delta_{\alpha}(\mathbf{i}, \mathbf{j}) c_{\mathbf{i}\uparrow}^{\dagger} c_{\mathbf{j}\downarrow}^{\dagger} + h.c., \quad (3)$$

where  $\Delta_{\alpha}(\mathbf{i}, \mathbf{j})$  is a mean-field superconducting order parameter. We focus on the unconventional sign-changed  $s_{+-}$  pairing symmetry so that  $\Delta_{\alpha}(\mathbf{i}, \mathbf{j}) = \Delta_0 \delta_{\mathbf{i}, \mathbf{j} \pm (\hat{x} \pm \hat{y})}$ .<sup>5,18</sup> For a conventional  $s_{++}$  superconductor,  $\Delta_{\alpha}(\mathbf{i}, \mathbf{j}) = \Delta_0 \delta_{\mathbf{i}, \mathbf{j}}$ .

We can rewrite the Hamiltonian in the momentum space as  $H_0 = \frac{1}{N} \sum_{\mathbf{k}} \Psi_{\mathbf{k}}^{\dagger} \hat{h}_{\mathbf{k}}^0 \Psi_{\mathbf{k}}$ , where

$$\hat{h}_{\mathbf{k}}^0 = \xi_{\mathbf{k}}^i \hat{\alpha}^i \otimes (\hat{\tau}^3 \otimes \hat{\sigma}^0) + \Delta_{\mathbf{k}} \hat{\alpha}^0 \otimes (\hat{\tau}^1 \otimes \hat{\sigma}^0), \quad (4)$$

and  $\Psi_{\mathbf{k}}$  is an 8-dimensional Nambu spinor  $\Psi_{\mathbf{k}}^{\dagger} = [c_{\mathbf{k}1\uparrow}^{\dagger}, c_{\mathbf{k}2\downarrow}^{\dagger}, c_{-\mathbf{k}1\downarrow}, -c_{-\mathbf{k}1\uparrow}, c_{\mathbf{k}2\uparrow}^{\dagger}, c_{\mathbf{k}2\downarrow}^{\dagger}, c_{-\mathbf{k}2\downarrow}, -c_{-\mathbf{k}2\uparrow}]$  with  $c_{\mathbf{k}\alpha\sigma}$  being a Fourier transform of  $c_{\mathbf{r}\alpha\sigma}$ . The Pauli matrices  $\hat{\alpha}^i$ ,  $\hat{\sigma}^i$  and  $\hat{\tau}^i$  act on the orbital, the particle-hole and the spin spaces, respectively. Then, the order parameter  $\Delta_{\mathbf{k}} = \Delta_0 \cos k_x \cos k_y$  for  $s_{+-}$  pairing, and the dispersions  $\xi_{\mathbf{k}}^0 = (t_1 + t_2)(\cos k_x + \cos k_y) + 4t_3 \cos k_x \cos k_y - \mu$ ,  $\xi_{\mathbf{k}}^1 = 4t_3 \sin k_x \sin k_y$ ,  $\xi_{\mathbf{k}}^2 = 0$ , and  $\xi_{\mathbf{k}}^3 = (t_1 - t_2)(\cos k_x - \cos k_y)$ .

The second term in the Hamiltonian  $H_{\text{mag}}$  describes the effects of the magnetic field and the SOC. In our work, we consider the out-of-plane magnetic field  $h_{\text{ext}}$ , and the Rashba-type SOC<sup>19</sup> with an angular momentum  $\mathbf{L}(\mathbf{k}) = (-\sin k_y, \sin k_x, 0)$ <sup>20,21</sup> on the two-dimensional  $x-y$  plane. Then, we have  $H_{\text{mag}} = \frac{1}{N} \sum_{\mathbf{k}} \Psi_{\mathbf{k}}^{\dagger} \hat{h}_{\mathbf{k}}^{\text{mag}} \Psi_{\mathbf{k}}$ , where

$$\hat{h}_{\mathbf{k}}^{\text{mag}} = -h_{\text{ext}} \hat{\alpha}^0 \otimes (\hat{\tau}^0 \otimes \hat{\sigma}^3) + v \hat{\alpha}^0 \otimes (\hat{\tau}^3 \otimes \mathbf{L}(\mathbf{k}) \cdot \hat{\sigma}) \quad (5)$$

with  $v$  being the strength of the SOC.

Here, we treat the magnetic impurity as a localized spin in the classical limit ( $S \gg 1$ )<sup>22-25</sup>, and the quantum (Kondo) effect of impurity is not under our consideration. In this limit, the magnetic impurity is equivalent to the local magnetic moment  $\mathbf{S}$ . Then the impurity Hamiltonian describes the interaction between the conduction electrons and the impurity spin located at  $\mathbf{r} = 0$

$$H_{\text{imp}} = \sum_{\alpha} \mathbf{S} \cdot (J_1 \mathbf{s}_{\alpha\alpha}(0) + J_2 \mathbf{s}_{\alpha\bar{\alpha}}(0)), \quad (6)$$

where  $J_1$  and  $J_2$  are the intra- and inter-orbital exchange couplings, and the operators  $\mathbf{s}_{\alpha\beta}(\mathbf{i}) = \frac{1}{2} \sum_{\sigma\sigma'} c_{\mathbf{i}\alpha\sigma}^{\dagger} \hat{\tau}_{\sigma\sigma'} c_{\mathbf{i}\beta\sigma'}$ . Spin-rotational symmetry of the system enable us to choose the  $z$  axis of the spin degrees of freedom to point in the direction of  $\mathbf{S}$ . We shall consider the effects of the intra-orbital impurity scattering, thus the strength of the impurity is given by  $w = S_z J_1$ . Using the Nambu spinor  $\Psi_{\mathbf{k}}$ , the impurity Hamiltonian can be rewritten as  $H_{\text{imp}} = \sum_{\mathbf{k}, \mathbf{k}'} \Psi_{\mathbf{k}}^{\dagger} \hat{V} \Psi_{\mathbf{k}'}$  with  $\hat{V} = J_1 S \hat{\alpha}^0 \otimes (\hat{\tau}^0 \otimes \hat{\sigma}^3) + J_2 S \hat{\alpha}^1 \otimes (\hat{\tau}^0 \otimes \hat{\sigma}^3)$ .

In our work, we perform a numerical study employing a mean-field  $T$ -matrix approximation<sup>4,26</sup>. In this case, we assume that the spatial variation of the superconducting order parameter can be neglected. Since the impurity interaction is limited to one site, scattering of quasiparticles from the impurity moment is described by a  $T$  matrix,  $\hat{T}(\omega)$  whose Fourier transform is independent of wave vectors. The single-particle Green's function for an impurity located at  $\mathbf{r} = 0$  is given by

$$\hat{G}(\mathbf{r}, \mathbf{r}'; \omega) = \hat{G}^{(0)}(0, \omega) + \hat{G}^{(0)}(\mathbf{r}, \omega) \hat{T}(\omega) \hat{G}^{(0)}(-\mathbf{r}', \omega), \quad (7)$$

where  $\hat{G}^{(0)}(\mathbf{r}, \omega) = \frac{1}{N} \sum_{\mathbf{k}} \hat{G}^{(0)}(\mathbf{k}, \omega) e^{i\mathbf{k} \cdot \mathbf{r}}$ . The single-particle Green's function for a clean system  $\hat{G}^{(0)}(\mathbf{k}, \omega) = [(\omega + i0^+)I - (\hat{h}_{\mathbf{k}}^0 + \hat{h}_{\mathbf{k}}^{\text{mag}})]^{-1}$ , where  $I$  is a 8-dimensional identity matrix. The Fermi surfaces in the presence of the SOC at zero magnetic field is presented in Fig. 1(b). The helicity bands remove the degeneracies of the electron spin in the electronlike and holelike pockets. With  $\hat{G}^{(0)}(\mathbf{r}, \omega)$  in hands, the  $T$  matrix can be obtained from the Lippmann-Schwinger equation

$$\hat{T}(\omega) = [\hat{V}^{-1} - \hat{G}^{(0)}(0, \omega)]^{-1}. \quad (8)$$

Note that as far as the spatial variation of order parameter can be neglected, these equations allow a complete solution of the problem.

The nature of the magnetic impurity induced bound states can be found by computing the spin-resolved local density of states (LDOS)

$$N_{\alpha\sigma}(\mathbf{r}, \omega) = -\frac{1}{\pi} \text{Im} G_{\alpha\sigma, \alpha\sigma}(\mathbf{r}, \mathbf{r}; \omega) \quad (9)$$

of which the poles give the energy spectra of single-particle excitations, and consist of those of the  $\hat{G}_0$  and the  $T$  matrix. The poles of  $T$  matrix signifies the appearance of the impurity induced states. It is known that a strong scattering yields localized states deep in the gap, while a weak scattering results in bound states close to the gap edge<sup>4</sup>.

For a quantum spin, one needs to address the Kondo effect<sup>27-29</sup>. However, here we treat the magnetic impurity with

a classical spin in a mean-field  $T$  matrix approximation approach. In this case the main effect of the exchange coupling between the local moment  $S$  and electron spin is the renormalization of the effective scattering potential for electrons of two different spin orientations, and so there are four impurity induced in-gap states, one for each electron-spin orientation in each  $d_{xz}$  ( $\alpha = 1$ ) and  $d_{yz}$  ( $\alpha = 2$ ) orbitals. It is noteworthy that the degeneracy between two orbitals are not broken by magnetic field and SOC as well, thus we omit the notation of  $\alpha$  in the spin resolved LDOS throughout this paper.

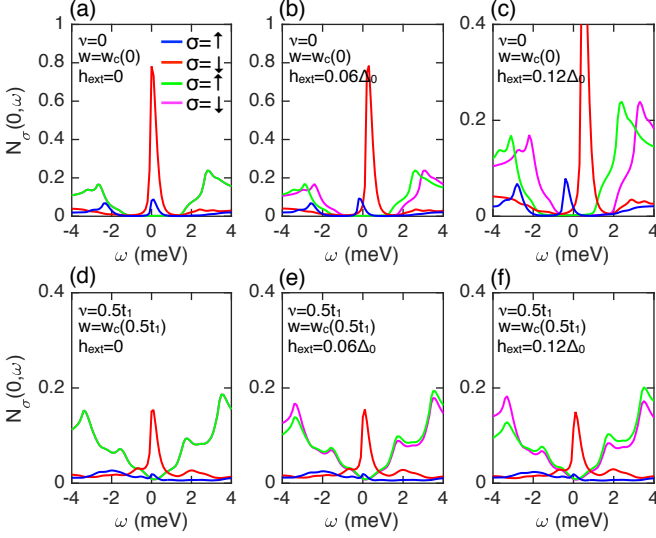


FIG. 2. Magnetic field and SOC effects on LDOS,  $N_\sigma$  for  $s_{+-}$  pairing vs bias energy  $\omega$  for clean system (green and magenta for  $\sigma = \uparrow, \downarrow$ , respectively) and system with an impurity at  $\mathbf{r} = 0$  (blue and red for  $\sigma = \uparrow, \downarrow$ ) at  $T = 1.5$  K. (a) and (d) show the appearance of both ZBPs for  $\sigma = \uparrow$  and  $\downarrow$  at the critical values  $w = w_c(\nu = 0)$  and  $w = w_c(\nu = 0.5t_1)$ , respectively; (b) and (c) illustrate the Zeeman splitting of  $N_\uparrow$  and  $N_\downarrow$  at weak magnetic fields  $h_{\text{ext}} = 0.06\Delta_0$  and  $0.12\Delta_0$  with no SOC. Whereas (e) illustrates the robustness of the ZBPs,  $N_{\uparrow, \downarrow}$ , to the applied magnetic field in the presence of SOC,  $\nu = 0.5t_1 = 5$  meV, (f) the Zeeman split begins to appear with increasing magnetic field for a single impurity in the system. Comparing the LDOS for clean systems (green and magenta), it is manifest that SOC slightly changes the low energy states by forming a V-shaped LDOS, and make the system robust against magnetic field.

We begin with the effects of the applied magnetic field and the SOC on the in-gap bound states induced by a single magnetic impurity for the sign changed  $s_{+-}$ -wave iron-based superconductor. Fig. 2 presents the spin-resolved LDOS  $N_\sigma(\mathbf{r} = 0, \omega)$  at the critical values of impurity strengths  $w = w_c(\nu = 0)$  and  $w = w_c(\nu = 0.5t_1)$  for a finite temperature  $T = 1.5$  K below the superconducting critical temperature  $T_c$ . For a weak impurity scattering  $w < w_c$ , the ground state has time-reversed pairs of single-particle in-gap states  $\pm\Omega$ , and as  $w$  increases, the energy  $\Omega$  approaches the chemical potential and, eventually, at the critical scattering strength  $w = w_c$ , it becomes a zero energy state, or zero-energy bound state (ZBS)<sup>2-5</sup>. Fig. 2(a) and (d) show the ZBSs for both spins ( $\sigma = \uparrow$  and  $\sigma = \downarrow$ ) with zero magnetic field applied,  $h_{\text{ext}} = 0$ . In the absence of the SOC ( $\nu = 0$ ), the corresponding zero

bias peaks (ZBPs) in the LDOS at  $h_{\text{ext}} = 0$  begin to split with increasing magnetic field  $h_{\text{ext}}$ . Fig. 2(b) and (c) illustrate the Zeeman splitting by the applied magnetic fields  $h_{\text{ext}} = 0.06\Delta_0$  ( $\sim 4$  Tesla) and  $h_{\text{ext}} = 0.12\Delta_0$  ( $\sim 8$  Tesla), respectively. In contrast, the presence of the SOC ( $\nu = 0.5t_1 \sim 5$  meV) dramatically reduces the Zeeman splitting and makes the ZBPs robust to the magnetic field [Fig. 2(e) and (f)]. It is noteworthy that the zero energy bound states localized at the impurity site in the presence of SOC remain pinned to zero energy even in a magnetic field  $0.12\Delta_0 \sim 8$  Tesla. It is in good agreement with the experimental observations<sup>1</sup>. We believe that the robust ZBSs is a strong signature of the presence of the SOC in the system. Note, however, the low energy quasiparticle states inside the gap in the clean system (green and magenta) even at  $h_{\text{ext}} = 0$  [Fig. 2(d),(e),(f)]. They exist because with a finite SOC  $\nu = 0.5t_1 = 5$  meV, the system is a nodal superconductor. Below we will show that in a system with a finite concentration of magnetic impurities as in the experiments<sup>1</sup>, the low energy quasiparticle density can naturally arise from Shiba states bound to the nearby impurities. In this case, the ZBSs localized at impurity sites are robust to applied magnetic fields (as well as to variations in the impurity potential) even for smaller values of SOC ( $\nu = 0.25t_1 = 2.5$  meV), corresponding to which the clean system has a full gap. This demonstrates that our results are robust and do not depend on the specific values of the parameters, as long as there is SOC and a finite concentration of low energy quasiparticles at the impurity sites as in the experiments.

Theoretically the robustness of the ZBS due to SOC can be understood to be due to a combination of suppression of the superconducting gap by SOC in the  $s_{+-}$  case and the properties of magnetic impurities in nearly isotropic gap superconductors. As seen in Fig. 1, SOC produces a relatively large spin splitting that pushes one Fermi surface towards the X-point and the other towards the  $\Gamma$ -point. On the other hand, in  $s_{+-}$  pairing, the pairing potential changes sign between these two points in the Brillouin zone. Therefore, as one Fermi surface moves towards the X-point, the pairing amplitude is suppressed, so that one of the Fermi surfaces would have a smaller gap. This suppressed gap is still quite isotropic and as shown in the appendix, for such isotropic Fermi surfaces, one can prove that an infinitesimal magnetic impurity will support sub-gap states just as in the case of the Shiba problem. However, if the gap is suppressed by SOC, then the impurity-induced sub-gap state is pinned to live inside the smaller gap, even in the presence of a magnetic field, explaining the robustness of the zero bias peak to Zeeman splitting. Since the coherence peaks from the larger gapped Fermi surfaces are expected to be larger, the smaller gap could appear as a pinned peak inside a larger gap.

Now we consider the robust ZBSs induced by the multiple magnetic impurities for  $s_{+-}$ -wave superconductor in the presence of SOC. This addresses the so-called class-D anti-localization mechanism. The case of a large number of bound states to magnetic impurities in a superconductor with SOC is described by random-matrix theory in symmetry class D. This symmetry class shows no level repulsion at zero energy. Because of this, the disorder averaged density of states (or the



density of states of a large number of weakly localized bound states) is expected to show a peak at zero energy quite generically independent of the magnetic field. Specifically, in the present context, nearby multiple Shiba impurities provide a second mechanism (aside from SOC) of reducing the magnitude of local gap near a given magnetic impurity. By the argument given in the appendix, the zero bias peak at the given impurity will then stay pinned at zero energy even if the value of the SOC is smaller, provided there is overlap of wave functions from states localized at nearby impurities. This demonstrates that our results are robust to specific values of SOC. Below we explore this mechanism numerically by introducing multiple Shiba impurities.

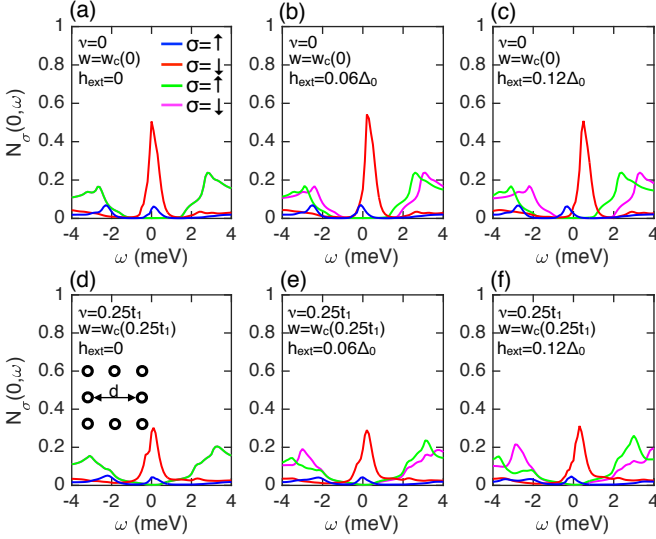


FIG. 3. Magnetic field and SOC effects on LDOS,  $N_\sigma$  for  $s_{+-}$  pairing vs bias energy  $\omega$  for clean system (green and magenta for  $\sigma = \uparrow, \downarrow$ , respectively) and system with multiple impurities (blue and red for  $\sigma = \uparrow, \downarrow$ ) at  $T = 1.5$  K. 8 impurities are located in a square and  $d = 12$  atomic sites. The LDOS are calculated at a impurity site. (a)–(c) show the ZBPs for  $\sigma = \uparrow$  and  $\downarrow$  at the critical value of the impurity potential with no SOC,  $w = w_c(\nu = 0)$ . The ZBP is split by applying magnetic field  $h_{\text{ext}} = 0.12\Delta_0$ ; (d)–(f) illustrate the robustness of the ZBPs,  $N_{\uparrow, \downarrow}$  in the presence of SOC,  $\nu = 0.25t_1 = 2.5$  meV.

For numerical analysis, we consider 8 impurities arranged in the shape of a square with the nearest neighbors separated by  $d/2 = 6$  lattice sites (various other arrangements of impurities give qualitatively the same results). For the multiple impurity problem, the Green's function, Eq. (7), is modified to include the scattering from the neighboring impurities  $\mathbf{r}_i$ .

$$\hat{G}(\mathbf{r}_i, \mathbf{r}_j; \omega) = \hat{G}^{(0)}(0, \omega) + \sum_{\delta \mathbf{r}_j} \hat{G}^{(0)}(\delta \mathbf{r}_j, \omega) \hat{T}(\delta \mathbf{r}_j, \omega) \hat{G}^{(0)}(-\delta \mathbf{r}_j, \omega), \quad (10)$$

where  $\delta \mathbf{r}_i = \mathbf{r}_i - \mathbf{r}_j$  runs for all impurities in the system, and  $\hat{T}(\delta \mathbf{r}_j, \omega) = [V^{-1} - G^{(0)}(\delta \mathbf{r}_j, \omega)]^{-1}$  is the  $8 \times n_{\text{imp}}$  matrix with  $n_{\text{imp}}$  being the number of the neighboring impurities. In Fig. 3, we present the spin-resolved LDOS  $N_\sigma(0, \omega)$  at one of the impurity sites ( $\mathbf{r}_i$ ) for clean system (green and magenta lines)

and the impurity induced bound states at the critical scattering  $w_c$  (blue and red lines) with and without SOC. The Zeeman splitting in the absence of SOC is manifest in the shift of each spin component in the LDOS for the clean system with increasing Zeeman field, as shown in Fig. 3(b) and (c). As the Zeeman field increases, the degeneracy between the two spin components is removed, thus  $N_\uparrow$  and  $N_\downarrow$  split from each other. On the other hand, even a weak SOC ( $\nu = 0.25t_1$ ) dramatically changes the zero energy bound states, maintaining the ZBPs even in the presence of the applied magnetic field  $\sim 8$  Tesla. Fig. 3(d) shows the appearance of the ZPBs at the critical value of the impurity scattering  $w = w_c(\nu)$  in the presence of a SOC  $\nu = 0.25t_1$  with no magnetic field applied. Fig. 3 (e) and (f) illustrate the robustness of the ZBPs to the magnetic field  $h_{\text{ext}}$ .

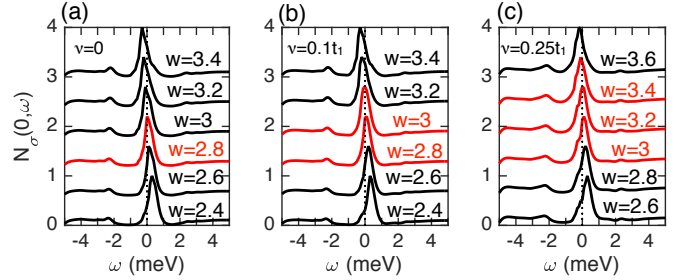


FIG. 4. SOC effects on the ZBP for  $s_{+-}$  pairing at  $h_{\text{ext}} = 0$  with 8 impurities in a square shape as in Fig. 3. (a) For  $\nu = 0$ , the ZBP appears at the critical value of impurity strength  $w = w_c(\nu = 0)$ . (b) and (c) show the ZBP remains in a range of impurity strengths and the robustness increases with increasing SOC.

In addition to robustness to applied magnetic field, in the presence of SOC and low energy quasi-particle states within the gap, the ZBPs in  $s_{+-}$ -wave superconductors also become robust to variations in the magnitude of the impurity scattering potential. This is important because without the SOC the appearance of the ZBP at magnetic impurity sites in  $s_{+-}$  superconductors requires fine tuned scattering potential at criticality  $w_c(\nu = 0)$ <sup>5</sup>. In contrast, the SOC maintains the appearance of ZBP in a range of magnetic impurity scattering potential above the critical value  $w = w_c(\nu)$ . Fig. 4 (b) and (c) show that the presence of the SOC maintains the ZBPs in a broad range of the impurity strength, whereas in the absence of the SOC, a ZBP is allowed only at the critical impurity scattering  $w = w_c(\nu)$  [Fig. 4(a)]. In this figure, to illustrate the impurity strength dependence of the peak positions,  $N_\sigma$  is normalized by the height as  $\tilde{N}_\sigma = N_\sigma / \max(|N_\sigma|)$ .

In contrast to unconventional sign-changed  $s_{+-}$  pairing, magnetic impurity-induced ZBSs in conventional  $s_{++}$  pairing ( $s$ -wave gap of the same sign on both hole and electron pockets) is *not* robust to applied magnetic fields even in the presence of SOC. Fig. 5 shows the spin resolved LDOS  $N_\sigma$  at a given impurity site for a spin-orbit coupled superconductor ( $\nu = 0.25t_1$ ) with  $s_{++}$  pairing ( $\Delta_{\mathbf{k}} = \Delta_0$ ) for various values of applied magnetic field and the magnitudes of impurity strengths. Fig. 5 (a) shows the appearance of the ZBS at  $w = w_c(\nu = 0.25t_1)$  at zero applied magnetic field and (b) shows the pronounced Zeeman splitting of the peaks even in

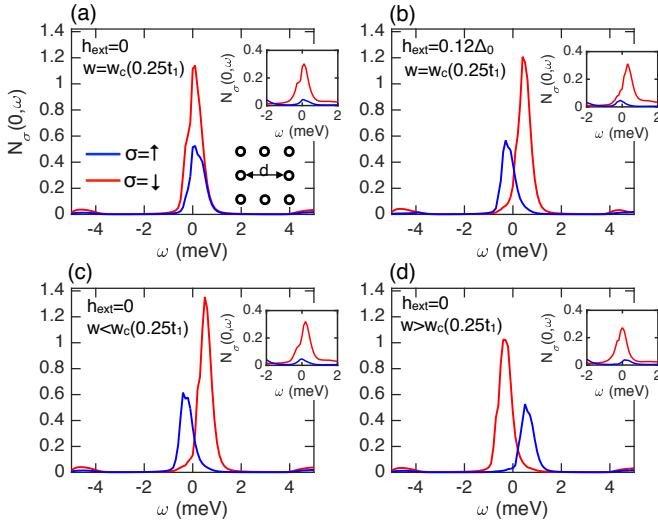


FIG. 5. Effects of magnetic field and impurity strength on the in-gap states for  $s_{++}$  pairing induced by 8 magnetic impurities in the presence of a SOC. (a) At  $w_c$ , the peaks for  $\sigma = \uparrow$  and  $\downarrow$  are located at zero bias  $\omega = 0$  for  $h_{\text{ext}} = 0$ . (b) Magnetic field splits into double peaks even in the presence of a SOC ( $\nu = 0.25t_1$ ). (c) and (d) illustrate the ZBPs are sensitive to values of impurity strengths at  $\nu = 0.25t_1$ . Insets illustrate the robustness of the ZBPs for  $s_{++}$  pairing against the magnetic field and impurity strengths at the same SOC strength,  $\nu = 0.25t_1$ .

the presence of SOC, which is in stark contrast to the case

of  $s_{+-}$  pairing as shown in the insets. It is noteworthy that the ZBSs for the  $s_{++}$  pairing requires fine tuning in the impurity potential even in the presence of SOC. Fig. 5 (c) and (d) show the double peak structure for  $\sigma = \uparrow$  and  $\sigma = \downarrow$  for  $w < w_c$  ( $\nu = 0.25$ ) and  $w > w_c$  ( $\nu = 0.25$ ), respectively, while the insets show the robustness of the ZBSs with SOC to variations in the magnitude of the impurity potentials for  $s_{+-}$  symmetry of the order parameter.

In summary, we have shown that robust zero energy bound states are induced at magnetic impurity sites in unconventional sign-changed  $s_{+-}$  superconductors in the presence of spin-orbit coupling. The robustness to magnetic fields and variations in the impurity scattering potentials are robust consequences of spin-orbit coupling along with low energy quasi-particle states within the superconducting gap, and do not require the existence of Majorana bound states on the surface of iron based superconductors. It is important to note that the zero energy bound states localized at magnetic impurity sites in conventional sign-unchanged ( $s_{++}$ ) superconductors remain sensitive to applied magnetic fields and variations in the impurity potentials even in the presence of SOC. Our results, in addition to providing a theoretical explanation of the puzzling observation of robust zero bias peaks in iron based superconductors described earlier as a serious theoretical challenge<sup>1</sup>, helps identifying the order parameter symmetry of these superconductors as sign-changing  $s_{+-}$  wave.

K.S and S.T are supported by AFOSR (FA9550-13-1-0045). J.D.S would like to acknowledge the University of Maryland, Condensed Matter theory center, and the Joint Quantum institute for startup support.

- <sup>1</sup> J.-X. Yin, *et. al.*, Nature Physics, **11**, 543 (2015).
- <sup>2</sup> A.V. Balatsky, M.I. Salkola, and A. Rosengren, Phys. Rev. B, **51**, 15547 (1995).
- <sup>3</sup> A. Yazdani, B. A. Jones, C. P. Lutz, M. F. Crommie, and D. M. Eigler, Science **275**, 1767 (1997).
- <sup>4</sup> A. V. Balatsky, I. Vekhter, and Jian-Xin Zhu, Rev. Mod. Phys., **78**, 373 (2006).
- <sup>5</sup> Wei-Feng Tsai, Yan-Yang Zhang, Chen Fang, and Jiangping Hu, Phys. Rev. B, **80**, 064513 (2009).
- <sup>6</sup> Y. Bang, H.-Y. Choi, and H. Won, Phys. Rev. B **79**, 054529 (2009).
- <sup>7</sup> J. Li and Y. Wang, Europhys. Lett. **88**, 17009 (2009).
- <sup>8</sup> A. Akbari, I. Eremin, and P. Thalmeier, Phys. Rev. B **81**, 014524 (2010).
- <sup>9</sup> T. K. Ng and Y. Avishai, Phys. Rev. B **80**, 104504 (2009).
- <sup>10</sup> M. Matsumoto, M. Koga, and H. Kusunose, J. Phys. Soc. Jpn. **78**, 084718 (2009).
- <sup>11</sup> D. Zhang, Phys. Rev. Lett. **103**, 186402 (2009).
- <sup>12</sup> T. Kariyado and M. Ogata, J. Phys. Soc. Jpn. **79**, 083704 (2010).
- <sup>13</sup> R. Beaird, I. Vekhter, and J.-X. Zhu, Phys. Rev. B **86**, 140507(R) (2012).
- <sup>14</sup> N. Read and D. Green, Phys. Rev. B **61**, 10267 (2000).
- <sup>15</sup> A. Y. Kitaev, Physics-Uspekhi **44**, 131 (2001).
- <sup>16</sup> E. Majorana, Nuovo Cimento **14**, 171 (1937).
- <sup>17</sup> S. Raghu, X.-L. Qi, C.-X. Liu, D. Scalapino, and S.-C. Zhang, Phys. Rev. B **77**, 220503 (2008).
- <sup>18</sup> K. Seo, B. A. Bernevig, and J. Hu, Phys. Rev. Lett. **101**, 206404 (2008).
- <sup>19</sup> Y. A. Bychkov and E. I. Rashba, J. Phys. C **17**, 6029 (1984).
- <sup>20</sup> L. P. Gorkov and E. I. Rashba, Phys. Rev. Lett. **87**, 037004 (2001).
- <sup>21</sup> P. A. Frigeri, D. F. Agterberg, A. Koga, and M. Sigrist, Phys. Rev. Lett. **92**, 097001 (2004).
- <sup>22</sup> L. Yu, Acta Physica Sinica **21**, 75 (1965).
- <sup>23</sup> H. Shiba, Progress of Theoretical Physics **40**, 435 (1968).
- <sup>24</sup> A. I. Rusinov, Soviet Journal of Experimental and Theoretical Physics Letters **9**, 85 (1969).
- <sup>25</sup> Jay D. Sau and Eugene Demler, Phys. Rev. B **88**, 205402 (2013).
- <sup>26</sup> F. Pientka, L. I. Glazman, and F. von Oppen, Phys. Rev. B **88**, 155420 (2013).
- <sup>27</sup> Polkovnikov, A., S. Sachdev, and M. Vojta, Phys. Rev. Lett. **86**, 296 (2001).
- <sup>28</sup> Zhang, G.-M., H. Hu, and L. Yu, Phys. Rev. Lett. **86**, 704 (2001).
- <sup>29</sup> Zhu, J.-X., and C. S. Ting, Phys. Rev. B **63**, 020506 (2001).
- <sup>30</sup> P. M. R. Brydon, S. Das Sarma, Hoi-Yin Hui, and Jay D. Sau, Phys. Rev. B **91**, 064505 (2015).

## Appendix A: Subgap states for weak coupling

Here we show that under quite generic circumstances there is always a sub-gap state bound to magnetic impurities. Bound states in a lattice are obtained by solving for the poles of the

T-matrix or the zeros of

$$H_{\text{eff}}(\omega) = V - G^{(0)-1}(\omega). \quad (\text{A1})$$

where in the case of a single-lattice site impurity,  $G^{(0)}(\omega)$  is calculated on one lattice site. In this case, the single-site Green function can be expanded in terms of BdG eigenstates of the bulk as

$$G^{(0)}(\omega) = \sum_{n,\mathbf{k}} \frac{\Psi_{n\mathbf{k}} \Psi_{n\mathbf{k}}^\dagger}{\omega - \epsilon_{n\mathbf{k}}} = \int d\epsilon \frac{\rho_0(\epsilon)}{\omega - \epsilon} \chi(\epsilon), \quad (\text{A2})$$

where  $\rho_0(\epsilon)$  is the DOS of BdG quasiparticles and  $\chi(\epsilon) = \rho_0(\epsilon)^{-1} \sum_{n,\mathbf{k}} \Psi_{n\mathbf{k}} \Psi_{n\mathbf{k}}^\dagger \delta(\epsilon - \epsilon_{n\mathbf{k}})$ .

Following Ref. 30, we note that in the presence of rotational symmetry about the  $z$ -direction the Green function

$[G^{(0)}(\omega), \sigma_z] = 0$ , so that it commutes with the impurity. In this case the two operators in the  $T$ -matrix can be simultaneously diagonalized and a bound state occurs whenever  $V = \lambda^{-1}$ , for some eigenvalue  $\lambda$  of  $G^{(0)}(\omega)$ . Since we are interested in weak impurities  $V$ , which could produce states at best at the gap edge, we ignore the energy dependence of  $\chi(\epsilon) \approx \chi_0$  and notes that the eigenvalues  $\lambda \approx f(\omega)\chi_{0,n}$ , where  $f(\omega) = \int d\epsilon \frac{\rho_0(\epsilon)}{\omega - \epsilon}$  is divergent and  $\chi_{0,n}$  are eigenvalues of  $\chi_0$ . Since  $\chi_0$  has at least one finite (non-zero) eigenvalue,  $\lambda^{-1} \propto f(\omega)^{-1} \rightarrow 0$  (as  $\omega \rightarrow \Delta_1$ ) where  $\Delta_1$  is the gap edge.

This implies that there is a bound state at arbitrarily small impurity strengths inside the spectral gap independent of how far the gap is suppressed. Near the gap edge, where in 2D,  $\rho_0(\epsilon)$  generically has a step function behavior at a minimum and a divergence in our (i.e. rotationally symmetric BCS) case one can approximate the energy dependence of  $\chi(\epsilon) \approx \chi_0 + \epsilon\chi_1$ .